energies

MDPI

Article

Energy-Efficient Speed Profile Approximation: An Optimal Switching Region-Based Approach with Adaptive Resolution

Jie Yang [1,2], Limin Jia [1,3,*], Shaofeng Lu [4], Yunxiao Fu [1,3] and Ji Ge [2,5]

1 State Key Laboratory of Rail Traffic Control and Safety, Beijing Jiaotong University, Beijing 100044, China; yangjie2013@bjtu.edu.cn (J.Y.); yunxiaof2012@163.com (Y.F.)
2 School of Electrical Engineering and Automation, Jiangxi University of Science and Technology, Ganzhou 341000, Jiangxi, China; gechunxi@126.com
3 Beijing Engineering Research Center of Urban Traffic Information Intelligent Sensing and Service Technologies, Beijing Jiaotong University, Beijing 100044, China
4 Department of Electrical and Electronic Engineering, Xi'an Jiaotong-Liverpool University, Suzhou 215123, Jiangsu, China; Shaofeng.Lu@xjtlu.edu.cn
5 Department of Mechanical and Industrial Engineering, University of Toronto, Toronto, ON M5S 3G8, Canada
* Correspondence: jialm@vip.sina.com; Tel./Fax: +86-10-5168-3824

Academic Editor: Jihong Wang
Received: 31 July 2016; Accepted: 12 September 2016; Published: 22 September 2016

Abstract: Speed profile optimization plays an important role in optimal train control. Considering the characteristics of an electrical locomotive with regenerative braking, this paper proposes a new algorithm for target speed profile approximation. This paper makes the following three contributions: First, it proves that under a certain calculation precision, there is an optimal coast-brake switching region—not just a point where the train should be switched from coasting mode to braking mode. This is very useful in engineering applications. Second, the paper analyzes the influence of regenerative braking on the optimal coast-brake switching region and proposes an approximate linear relationship between the optimal switching region and the regeneration efficiency. Third, the paper presents an average speed equivalent algorithm for local speed profile optimization in steep sections. In addition, this paper simplifies the proof of the optimality of smooth running on a non-steep track in two steps. The effects on energy consumption from two important factors (optimal coast and running time) are systematically analyzed. Extensive simulations verify these points of view and demonstrate that the proposed approximation approach is computationally efficient and achieves sufficient engineering accuracy.

Keywords: energy consumption; speed profile approximation; adaptive resolution; simulation study

1. Introduction

As one of the most important means of transportation, the railway plays a significant role in the development of society. Rising energy prices and environmental concerns have placed great social, economic, and environmental value on the study of railway energy savings. Because traction systems represent more than half of the energy consumption, the problem of energy-efficient train operation has aroused significant interest. To obtain a satisfactory target speed profile for an automatic train operation system (ATO), based on existing results in train optimal control research, this paper discusses an optimal switching region-based approach with adaptive resolution.

1.1. Literature Review

Since the 1960s, many researchers have published numerous outstanding works on energy-saving techniques in railway engineering. A methodology tree can be generated as shown in Figure 1. Our approach to speed profile approximation is based on the research results concerning the maximum principle and heuristic algorithm.

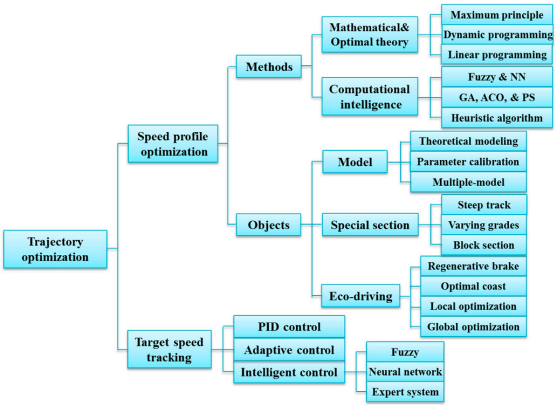

Figure 1. Methodology tree of energy-efficient train operation.

1.1.1. The Significant Milestones

Sidelnikov [1] proposed the driving strategy optimization problem. In 1982, led by Milroy, SCG (Scheduling and Control Group) was founded at the University of South Australia. Since then, the group has contributed significantly to the field of train modeling and operation strategy optimization. Group members Cheng et al. [2,3], Howlett et al. [4,5], Vu [6], and Albrecht et al. [7,8] systematically studied optimal strategies using mathematical approaches, and they laid a solid theoretical foundation in this area.

Khmelnitsky [9] attempted to solve the problem of optimal control by applying the maximum principle and co-state equations, which consider regenerative braking. Liu et al. [10] discussed the analytical solution that gives the optimal sequence of controls and equations to find the control change points. The drawback was that these approaches needed multi-round complex and time-consuming multi-variable optimizations.

1.1.2. Mathematical Methods and Optimal Theory

Considering the effect of regenerative braking, Lu [11] applied linear programming to search for the train braking trajectory that generates the maximum regenerative braking energy. Lu et al. [12,13] proposed a complete mathematical model in which a mixed-integer linear programming algorithm can be directly applied.

In addition, Miyatake et al. [14,15], Ho et al. [16], and Sheu et al. [17] performed productive research on mathematical approaches and optimal theory. Mathematical methods are based on accurate models, which are sometimes difficult to obtain. Thus, constraint simplifications and calculation errors are inevitable in most cases, but it is an effective way to search for solutions using the combined approach of mathematical analysis and computational intelligence. Scholars in this field have always been in the pursuit of analytical solutions by mathematical methods and optimal theory; however, in the case of complex line conditions such as varying slopes and long, steep tracks, an analytic solution in the mathematical sense is still unable to be obtained. Necessary simplifications and engineering treatments are always used to find a satisfactory solution.

Practical driver advice systems already operating on-board trains in real time using numerical methods are outlined in [4,7–10]. The Energymiser® currently being used in France on the famous TGV trains and elsewhere in the UK, Europe, Australia, and India is one such system.

1.1.3. Computational Intelligence

Yasunobu et al. [18] applied fuzzy logic to the study of train operation control in 1985 and successfully applied this technique in the design of an ATO system. Jia [19] and his team have been devoted to enhancing the technology of Chinese railway automation since the 1990s, attempting to model drivers' professional knowledge in machine language using fuzzy logic. They have successfully applied fuzzy prediction, two-level hierarchical intelligent control, and multi-objective optimizations to railway automation systems. Bai et al. [20] and some other researchers have also performed very important work on train intelligent control using fuzzy logic, which has unique advantages in describing complex deduction processes and is often combined with NNs (neural networks), GAs (genetic algorithms), etc. to improve its performance.

Researchers began to solve railway problems using GA in the 1990s. Chang et al. [21] applied a GA to solve the optimal train coasting problem. Wong et al. [22] applied a GA to search for the appropriate coasting points and investigated possible improvements to the fitness of genes. In addition, a hierarchical GA was introduced to identify the number of coasting points that were required according to the traffic conditions. Lu et al. [23] performed a study using changeable-chromosome-length multi-objective GA. Li et al. [24] set the energy consumption as a constraint of train operation to study the collaborative optimization problem of speed profiles and timetables. Huang et al. [25] used a multi-population GA to solve the driving strategy problem for multiple inter stations. Lin et al. [26] discussed the multi-train energy saving problem for maximum usage of regenerative braking in urban rail transit. GAs have the advantages of random search, potential parallelizability, and scalability and the disadvantages of slow searching, excessive changes in the control variables, and inevitable speed fluctuations. Thus, they too are often combined with other algorithms.

Moreover, many outstanding researchers have applied various other methods. Lu [11] performed a comparative analysis among GA, DP (dynamic programming), and ACO (ant colony optimization) and suggested that the robustness could be improved by combining different algorithms. Yin et al. [27] presented two intelligent train operation algorithms based on expert systems and reinforcement learning without precise train model information and offline optimized speed profiles. Domínguez et al. [28] used multi-objective particle swarm optimization to collaboratively optimize the running time, train speed, and energy consumption.

In summary, models are the foundation of train operation optimization. Because train operation has many constraints and some parameters change over time, certain dynamics are still difficult to model. The energy consumption mechanism is too complex to be completely modeled. To meet the dynamic and multi-objective requirements of railway engineering, this paper proposes a new method of speed profile optimization; based on this, some interesting simulations are conducted.

1.2. Main Contents

Taking references from drivers' manual operation, we believe that it is feasible to realize high-performance eco-driving using the technology roadmap of offline optimal speed profile programing $\rightarrow$ online data acquisition $\rightarrow$ multi-objective online speed profile optimization $\rightarrow$ train speed online tracking.

The remainder of this paper is organized as follows. Section 2 presents the problem statement of this paper and introduces the framework of our speed profile optimization algorithm. Before we introduce the algorithm, we discuss the optimal strategy on a non-steep track in two steps in Section 3, and some simulations are performed in Section 4 to prove, with certain computational accuracy, that there is an optimal region, not just a point, in which trains should be switched from the coasting mode to the braking mode. We then study the approximate linear model between the optimal switching region and the braking energy regeneration efficiency of regenerative braking. The influence of running time on energy consumption is also analyzed in Section 4. Section 5 elaborates on the speed profile optimization algorithm. The case study is presented in Section 6, and conclusions are provided in Section 7.

2. Problem Description

2.1. Problem Statement

Generally speaking, energy consumption in a railway system can be divided into traction and non-traction energy consumption, and more than 70% of the energy consumption of a freight train is spent in the traction system, especially for heavy-haul trains [29].

The current key point of the optimal train control problem is to propose a fast and efficient algorithm for speed profile optimization that can determine a satisfactory speed profile based on given conditions including running time, travel distance, train formation, and line details. Considering the characteristics of both the mechanical system and the electrical system, the most important point is that the optimized speed profile be implementable. For the actual situation of nonlinear and multi-constraint systems, it is always difficult to obtain a theoretically optimal solution. A suitable trade-off between computational accuracy and computational speed should be found.

2.2. An Illustration of Excellent Train Drivers

Excellent experienced drivers can flexibly address all types of complex conditions and reasonably respond to various perturbations and interruptions. The robustness of the human brain is the key missing factor in automatic driving systems.

If we carefully analyze the driver operation process, it can be noticed that the decision-making process can be understood as a three-level hierarchical dynamic optimization process. In the first level, the running time of every mode is roughly distributed, and the speed profile's outline is sketched before starting the trip. In the second level, the speed profile section is refined by section based on line details of the track gradient, curve radius, length of the tunnel, and other influencing factors of the force analysis. In the third level, the difference between the offline speed profile and the actual velocity-distance-time relationship is dynamically detected during the driving process, and the driving strategies are then dynamically adjusted based on the driver's knowledge and driving experience.

2.3. Speed Profile Approximation Framework

We propose the speed profile programing framework shown in Figure 2 to solve the problem of approximation with multiple constraints.

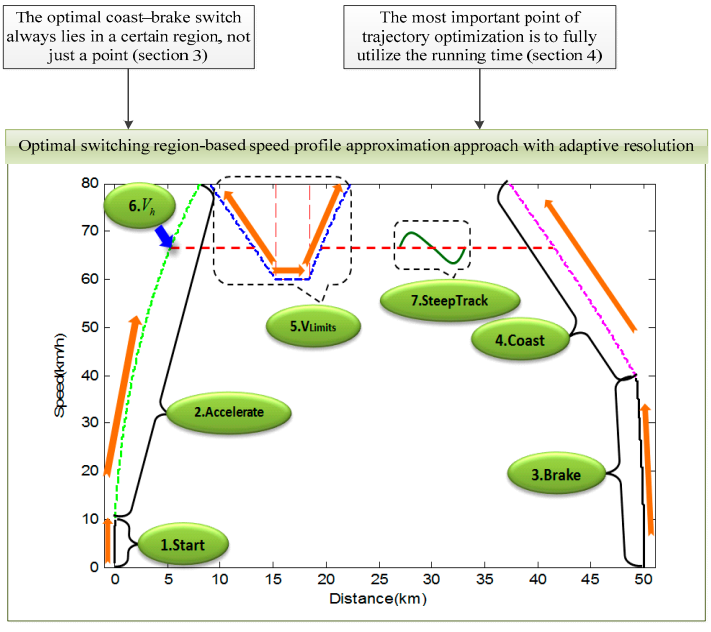

Figure 2. Framework of speed profile optimization.

3. A Simplified Optimal Speed Profile Model on Non-Steep Track

An eco-driving strategy is a complex multi-constraint problem, which is difficult to solve analytically through mathematical approaches. It is helpful to find a satisfactory solution via some simplification. The operating conditions can be simplified to an ideal short journey, as systematically discussed by Milroy in 1980 and Tyler in 1982. The research achievements showed that the journeys have four phases: maximum acceleration, speed hold, coast, and maximum brake. Thus, the speed profile optimization on level track is in fact a problem of Switching Point (SP) searching.

There are three types of switching points on a level track: Acceleration–Hold Switching Point (AHSP), Hold–Coast Switching Point (HCSP), and Coast–Brake Switching Point (CBSP). AHSP is relatively easy to locate based on the proper acceleration rate and holding speed. Many strategies (pairs of V_h (holding speed) and CBSP) can be achieved using 2-dimensional enumerations based on a given running time and distance. Each strategy corresponds to a speed profile in Figure 3.

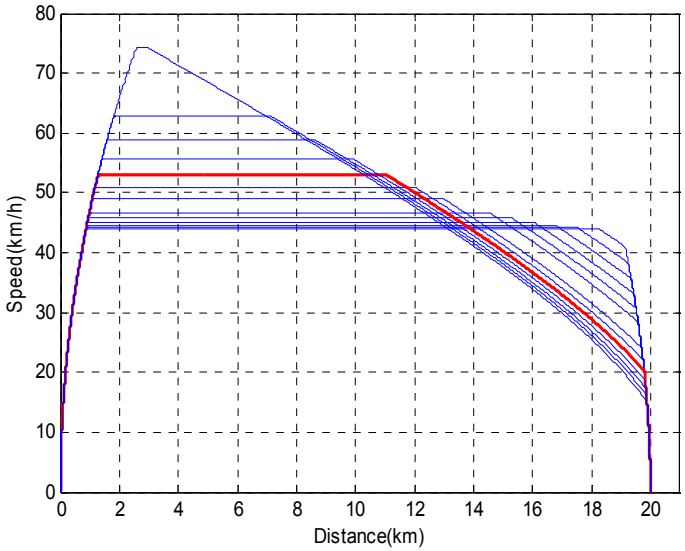

Figure 3. Comparison chart of operation strategies with different V_h and switching points.

There must be a strategy among them with minimal energy consumption, which can be determined by accumulating the energy consumption of every time step of every strategy according to Appendix A. However, this is computationally demanding. We need a more efficient algorithm to find the optimal strategy.

Howlett [4] determined the optimal coast (the relationship between CBSP and holding speed V_h) for non-steep track. We believe that it is mathematically intensive for understanding and engineering applications. Here, we simplify the proof in two steps. First, we deduce the optimal coast equation for ideal level track in Section 3.1. We then prove that the optimal strategy for non-steep track is the same as that of level track in Section 3.2.

3.1. Optimal Coast on Level Track

As shown in Figure 3, the shape of the speed profile is determined by the holding speed V_h and the CBSP speed V_b. Some related parameters used in the derivation equation to obtain the optimal relationship between V_h and V_b are listed in Table 1.

Table 1. Subscripts, parameters, and variables used in the mathematical formulations.

Symbol	Definition
$a(v,u)$	Acceleration per unit mass arc (v,u)
$B(u)$	Braking force per unit mass arc u
$e_{traction}(v,u)$	Traction energy consumption per unit mass arc (v,u)
$g_{slop}(x)$	Component of gravitational acceleration in the direction of motion
$r(v)$	Basic resistance per unit mass
u, u_q, u_p	Control input, maximum braking input, and maximum traction input
v	Speed of train
V_h	Holding speed
V_b	Speed of theoretically optimal CBSP where brake should be applied

Following the approach of Howlett [4], we set $g_{slop}(x) = 0$ for level track; in combination with the models in Appendix A, we have

$$a(v,u) = Ae_{traction}(v,u)/v + B(u) - r(v) \tag{1}$$

where $A > 0$ is constant. The Hamiltonian is given by

$$H(v,\alpha,\beta,u) = -e_{traction}(v,u) + \alpha v + \beta[Ae_{traction}(v,u)/v + B(u) - r(v)] \tag{2}$$

The adjoint equations are

$$\begin{cases} d\alpha/dt = 0 \\ d\beta/dt = -\alpha + \beta[Ae_{traction}(v,u)/v^2 + r'(v)] \end{cases} \tag{3}$$

Thus, the maximized Hamiltonian can be written as

$$H(u) = (A\beta/v - 1)e_{traction}(v,u) + \beta B(u) + \ldots \tag{4}$$

Equation (4) should also be considered in five different cases under discussion

$$\begin{cases} u = u_p & \beta > v/A \\ u \in (0, u_p) & \beta = v/A \\ u = 0 & 0 < \beta < v/A \\ u \in (u_q, 0) & \beta = 0 \\ u = u_q & \beta < 0 \end{cases} \tag{5}$$

Hence, the condition

$$\beta = v/A \tag{6}$$

corresponds to the speed holding mode, and it is the key to the optimal strategies.

By differentiating both sides of Equation (6) and rearranging it in combination with Equation (3), we have

$$a = \varphi'(v)/A \tag{7}$$

where $\varphi(v) = v \cdot r(v)$.

From Equation (3), we can see that α has a constant value C at the same time. Because $\varphi(v)$ is convex, the holding speed $v = V_h$ is followed by

$$e_{traction}(v,u) = \varphi(V_h)/A \tag{8}$$

The Hamiltonian is constant along the entire optimal trajectory; that is, $\mu = H(t)$. Therefore, we can substitute Equations (6) and (7) into Equation (2), and we will obtain

$$\mu = \psi(V_h)/A \tag{9}$$

where $\psi(v) = v^2 r'(v)$.

Suppose that the train coasts in $t \in [a, b]$, which means that the HCSP is $t = a$ with $V_h = v(a)$ until CBSP $t = b$ with $V_b = v(b)$. Thus, we can obtain $D(a, b) = 0$. From [4], we know that

$$\alpha_b - \alpha(a) = \mu \int_{s=a}^{b} \frac{de^{D(t,b)}}{v(t)} = 0 \tag{10}$$

where

$$D(a, b) = \int_{s=a}^{b} \frac{V(s) \cdot g'[x(s)]}{g[x(s)] - r[v(s)]} ds \tag{11}$$

By evaluating the Hamiltonian at $t = a$ and $t = b$, from Equations (7), (9), and (10), we can obtain

$$\alpha(a) = \varphi'(V_h)/A \tag{12}$$

$$\alpha_b = \mu / V_b \tag{13}$$

Thus, we obtain the same key equation about the holding speed V_h and the speed of CBSP V_b as

$$V_b = \psi(V_h)/\varphi'(V_h) \tag{14}$$

Based on this equation, the 2-dimensional iteration problem will be simplified to a question of seeking V_h, which can be easily solved. Once V_h and V_b are settled, AHSP and HCSP can be easily calculated using integration, and the theoretical optimal speed profile on an ideal level track can be drawn as the red line in Figure 3.

3.2. Optimal Train Operation on Non-Steep Track

In the previous sections, we considered train operation on level track with full power acceleration, speed holding, coasting, and braking with a maximum deceleration rate. Here, we will prove that the strategy for a trip on non-steep track is the same as on ideal level track.

3.2.1. Optimality of Speed Holding on a Non-Steep Track

A steep track includes two types of gradients: steep uphill and steep downhill. An uphill slope is said to be 'steep' if the train has insufficient power to maintain a desired constant holding speed on the slope, and a downhill slope is said to be 'steep' if the train increases its speed while coasting. All slopes between the steep uphill and steep downhill slopes are non-steep tracks on which the train could maintain its running speed by adjusting the traction force.

Suppose that train A travels on level track L_A and passes the section from x_1 to x_2 with a holding speed V_h, as shown in Figure 4a. The same train B travels on line L_B and passes the non-steep track (from x_1 to x_2) with the same holding speed, as shown in Figure 4b. Suppose that line L_A is the same as L_B except for the non-steep track from x_1 to x_2.

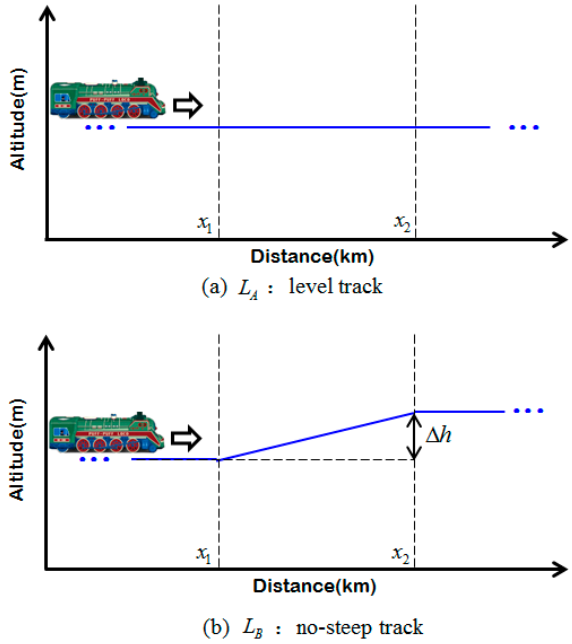

Figure 4. Train travelling on non-steep track compared with level track.

Calculate the energy consumptions in section x_1 to x_2 of train A and B as

$$E_A = F_A(x) \cdot (x_2 - x_1) = M \cdot \omega_0 \cdot (x_2 - x_1) \tag{15}$$

$$E_B = F_B(x) \cdot (x_2 - x_1) = M \cdot (\omega_0 + \omega_j) \cdot (x_2 - x_1) \tag{16}$$

The energy consumption caused by the basic resistance ω_0 is the same if the holding speeds are the same. Thus, the energy consumption caused by the additional resistance ω_j is

$$\Delta E = E_B - E_A = M \cdot \omega_j \cdot (x_2 - x_1) = M \cdot g \cdot \Delta h \tag{17}$$

As we can see, $\Delta E = M \cdot g \cdot \Delta h$ is the energy needed to overcome the forces due to gravity; thus, we can say that train B does not waste any extra energy except in overcoming basic resistance and gravity. Because an optimal strategy is for train A to pass the section with a holding speed, which is the same as running on a level track, passing a non-steep track at a holding speed is also an optimal strategy. Thus, we obtain Remark 1.

Remark 1. *For an electrical locomotive with constant energy efficiency on non-steep track, the optimal slope-passing strategy is to maintain the train speed.*

3.2.2. Optimal Switching Points on Non-Steep Tracks

According to Remark 1, for non-steep track, operating a train under the same strategies as on level tracks results in an energy consumption difference of $\Delta E = M \cdot g \cdot \Delta h$. Thus, we can arrive at Remark 2.

Remark 2. *For an electrical locomotive with constant energy efficiency on non-steep track, the optimal strategy is to maintain operating modes and switching points the same as on level track.*

4. Two Factors Affecting Energy Consumption

4.1. Optimal Coast-Brake Switching Region

Conventionally, optimal coast is one of the hottest topics of energy-efficient train operation. Here, using a simulation study, we will prove that considering the integration error and calculation accuracy, the optimal coast-brake switch always lies in a certain region, and not just a point.

4.1.1. Optimal Switching Region without Regenerative Braking

Reasonable coasting can shorten the traction distance and reduce operation energy consumption; however, excessive coasting at low speed will increase the running time and lead to increased total energy consumption. Theoretically, Equation (14) is the only optimal point for the train to switch from coasting mode to braking mode on level track without regenerative braking. A simulation study has been performed to prove that there is not necessarily one unique optimal solution from the viewpoint of engineering applications.

First, we define the CBSPs in Figure 3 as V_{CBSP_i}:

$$V_{CBSP\_i} = V_h - p_{cb} \cdot (V_h - V_b) \tag{18}$$

where p_{cb} is a parameter used to adjust the coasting range and V_b is the optimal speed at which to switch to braking, which we obtain from Equation (14).

We then iterate p_{cb} from 0% to 200% with a step size of 1% to obtain a set of V_{CBSP} and deduce the corresponding CBSP of a separate strategy for each V_{CBSP}. Energy consumption can be calculated for each case with different V_{CBSP}, as shown in Figure 5. When $p_{cb} > 153\%$, the iteration process will terminate for $V_{CBSP} \leq 0$, which means that no braking will occur.

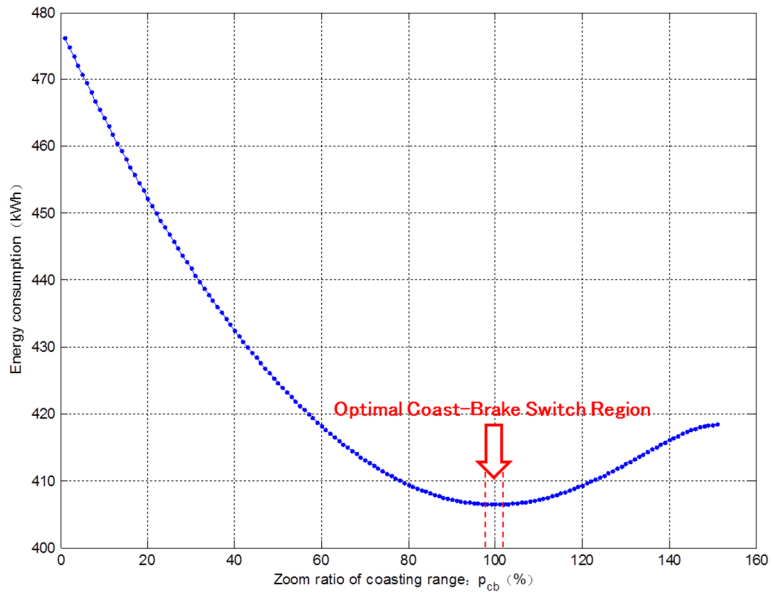

Figure 5. Energy consumption change over different coasting ranges.

According to SCG's mathematical analysis, minimal energy consumption would occur only at $p_{cb} = 100\%$. Figure 5 shows that energy consumption changes little during $93\% \leq p_{cb} \leq 106\%$, especially during $98\% \leq p_{cb} \leq 102\%$, where the energy consumption remains very close to 406.48 kWh. The energy consumption changes by no more than 0.1 kWh, accounting for less than 0.03% of the total energy consumption (desirability function $\mu_e(\Delta p_{cb}) = 99.97\%$). Thus, two remarks can be given:

Remark 3. *Considering the integration error and calculation accuracy, optimal coast strategies always lie in a certain region, not just a point. We call this region the "optimal coast-brake switching region" with a desirability function* $\mu_e(\Delta p_{cb})$.

Remark 4. *Even if there is a difference between the theoretically optimal point and the optimal region in remark 3 when the integration error is eliminated through a huge amount of computation, it would be negligibly small for engineering applications.*

These two remarks are critical for some necessary adjustments in engineering applications, especially in applications where positioning accuracy is not accurate enough.

4.1.2. Optimal Switching Region with Regenerative Braking

The regenerative energy feedback is not considered in the simulation of Figure 5, which means that it is a special case of braking energy regenerative efficiency $p_{reg} = 0$. Taking $\Delta p_{reg} = 0.01$ as the step size, we can obtain a three-dimensional image as shown in Figure 6, which visually demonstrates the effects on energy consumption of p_{reg} and p_{cb}.

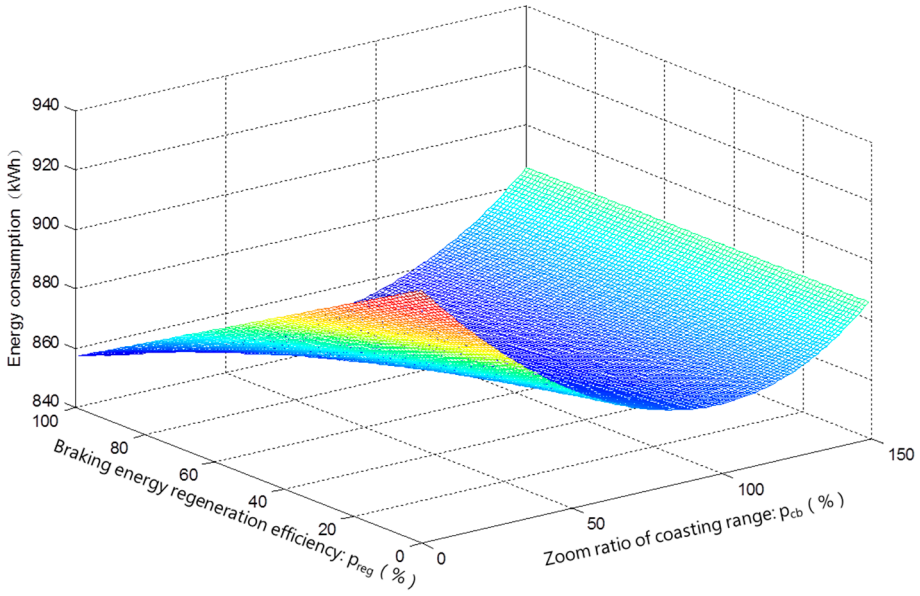

Figure 6. Comparison diagram of changing energy consumptions with p_{reg} and p_{cb}.

In Figure 6, we can see the 3D effect of how energy consumption changes over different braking energy regenerative efficiencies p_{reg} and coasting ranges p_{cb} (CBSP is determined by p_{cb} according to Equation (18)). If we increase the step size of Figure 6 (take $\Delta p_{reg} = 0.1$) and sketch the figure in a 2D chart, 11 curves can be drawn as shown in Figure 7.

As shown in Figure 7, for certain p_{reg}, the bottom regions of the corresponding energy consumption curves are very flat in support of Remark 4.

Taking the corresponding energy consumption curves of $p_{reg} = 0.5$ in Figure 7 as an example, the energy consumption changes by no more than 0.5 kWh during CBSP changes within the range of $80\% \leq p_{cb} \leq 90\%$, accounting for less than 0.06% of the total energy consumption. In particular, within the range of $84\% \leq p_{cb} \leq 88\%$, the difference is negligible.

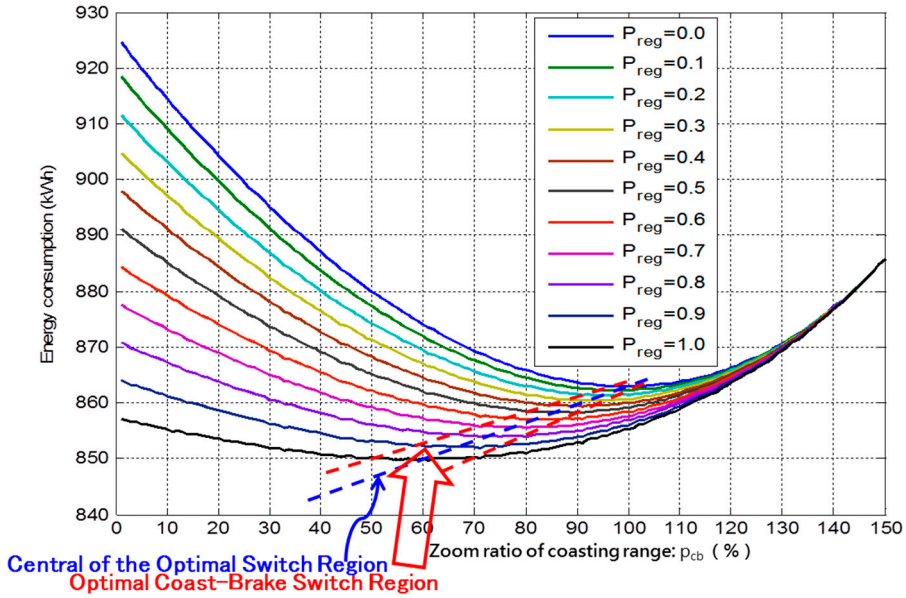

Figure 7. Approximate linearization of the optimal coast-brake switching region.

Meanwhile, the optimal coast-brake switching region has fairly good linear characteristics. As a result, the optimal switching center and the width may be approximately linearized as

$$V_{CBSP\_r} = V_h - (1 - 0.4 \cdot p_{reg}) \cdot (V_h - V_b) \tag{19}$$

$$\Delta p_{cb} = \pm(5 + 5 \cdot p_{reg}) \tag{20}$$

4.2. Influence of Running Time on Energy Consumption

For a given distance, different scheduled running times will result in different operation strategies and thus corresponding speed profiles. In the following simulation, on a 20 km level track, the different running times and corresponding optimal speed profiles are shown in Figure 8. Note that the relationship between the value of the holding speed and the CBSP is derived based on Equation (14).

Simulation steps:

Step 1: According to the given distance, deduce the minimal running time and its corresponding speed profile, which follows Equation (14). This means that the train runs with full power and then switches from acceleration mode directly to coasting mode, as demonstrated by the red curve in Figure 8.

Step 2: Increase the running time with a step size of 100 s and deduce the corresponding speed profile.

Step 3: Execute step 2 iteratively until the outline of the latest speed profile changes within an acceptable range.

Step 4: Plot the speed profiles of all of the above steps, as shown in Figure 8.

Similarly, for a given distance, strategies with different running times cost different amounts of traction energy. We summarize the corresponding energy consumptions of Figure 8, as shown in Figure 9, within which the regenerative braking energy is not considered. Each circle in Figure 9 indicates the energy consumption of an operation strategy (speed profile) in Figure 8.

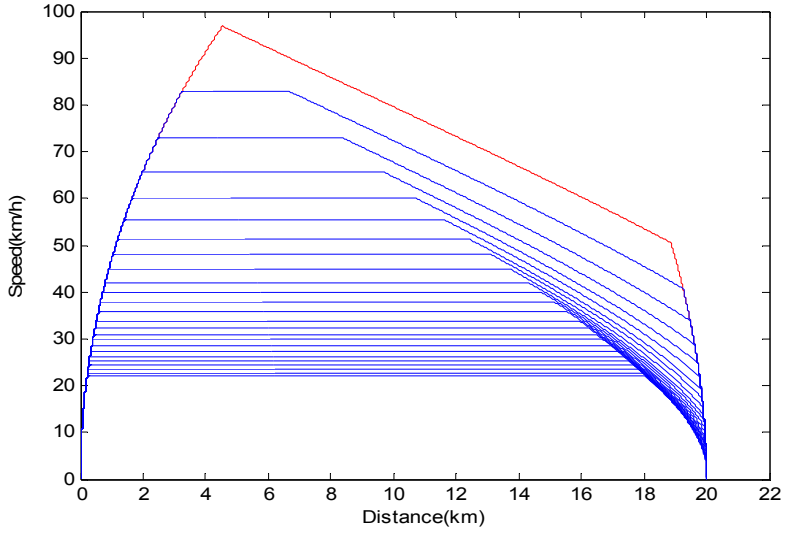

Figure 8. Equidistant speed profiles with various running times.

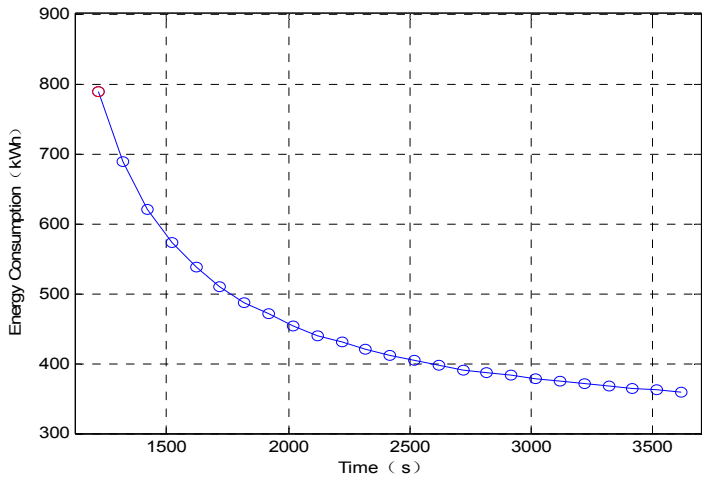

Figure 9. Energy consumptions for various operation strategies with different running times.

As shown in Figure 9, the running time obviously affects the energy consumption. For example, from t = 1600 s to t = 1800 s, the energy consumption difference is up to 50 kWh, which means that approximately 0.25 kWh of energy consumption can be saved for every additional second of running time.

By comparing the simulations and discussions in Sections 4.1 and 4.2, we can see that the running time influences the traction energy consumption substantially more than the optimal coast. The most important aspect of energy-efficient train operation is to fully utilize the running time.

5. Adaptive Resolution of Speed Profile Approximation

As shown in the framework (Figure 2), the optimization of the speed profile can be roughly divided into 7 steps. To make the process more easily understood, we present the simulation processes, as shown in Figure 10.

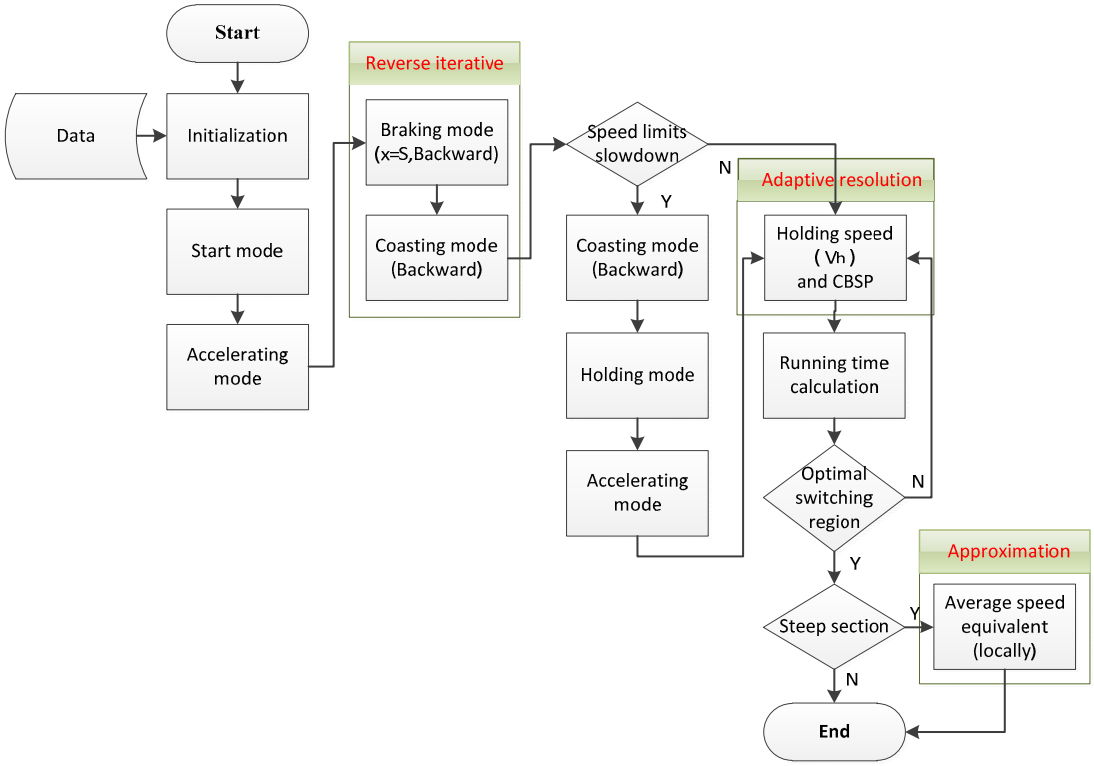

Figure 10. Simulation process of speed profile optimization.

(1) Upload required data (e.g., speed limits, gradients, curves, tunnels, train formation, mass, length, running time, distance, traction characteristics, braking characteristics, and step size).

(2) Switch to start mode until the end of the train begins to move forward at a low speed. Then switch to accelerating mode and increase the speed until the maximum speed limit is achieved (always 80 km/h in China) (see Section 5.1).

(3) To fully utilize the scheduled running time and ensure the accuracy of parking, derive the braking process from the parking point using a reverse iterative. Then derive the coasting process from CBSP using a reverse iterative until the train speed reaches the speed limit (see Section 5.2).

(4) If there are sections in which the speed limit is lower than in the former section, insert a set of coasting–holding–accelerating modes (see Section 5.3).

(5) To filter out part of the invalid control output alternatives and reduce the number of calculations, draw a speed–ceiling profile which means that the train runs as fast as possible and travels with a minimal running time (see Section 5.4).

(6) Find a proper holding speed V_h by adaptive resolution, set it as the cruise speed, cut the overshoot, and calculate the corresponding running time. Then, analyze whether the CBSP is within the optimal switching region (see Section 5.5).

(7) Draw a speed reference profile considering of all operating constraints, except the tractive force limitation on steep slopes. (see Section 5.6).

(8) Approximate the speed profile of steep track sections locally using the average speed equivalent algorithm (see Section 5.7).

5.1. Start and Accelerating Modes

A smooth start is preferred for a freight train, and a slow speed should be maintained until the end of the train begins to move. Jerk avoidance control must consider the train formation and the characteristics of the locomotive's mechanical and electronic systems.

In the accelerating mode, it is necessary to limit the acceleration according to the constraints (see Appendix B) to ensure that the coupler force is within the safety range and under an acceptable jerk rate.

5.2. Coasting and Braking Modes

From Figure 9 and the corresponding analysis in Section 4.2, it can be concluded that one of the key aspects of energy savings is to fully utilize the scheduled running time.

Therefore, the algorithm calculates the braking curve backward from the parking point and then the coasting curve to ensure that the parking point precisely matches the constraints of the running time and distance.

The equation of the backward iteration is

$$s_i = s_{i-1} - v_i \cdot \Delta t \tag{21}$$

Here, the CBSP should be determined according to Equation (14).

Regarding the online optimization, however, flexible CBSP adjustments can be made within the optimal switching region determined by Equations (19) and (20) to fully utilize the running time and to stop precisely at train stations without a huge increase in computational time.

5.3. Speed Limit Slowdown

A train must coast in advance when the speed limit decreases in some sections. There are two methods to precisely locate the HCSP: one is by integration, and the other is by bidirectional iteration.

Using the first method, we must find the location x_{HCSP} that satisfies the equation

$$V_{h0} = V_h - \int_{x=x_{HCSP}}^{x_0} a(x)dx = V_h - \int_{x=x_{HCSP}}^{x_0} \frac{c(x)}{M}dx \tag{22}$$

As observed in Appendix A, $c(x)$ changes along the distance x and speed $v(x)$ because the resistance force varies with speed $v(x)$, gradients, curves, etc. Thus, the integral is computationally quite complex. On the other hand, a bidirectional iteration algorithm is fairly simple and adaptive for various line conditions.

Thus, first, perform the iterative computation without the coasting operation in advance, and record the speed data until the train speed exceeds the reduced speed limit: $v(x_0) > v(x_{\max})$.

Then, deduce x_{HCSP} from x_0 via backward iteration based on Equation (21).

When the speed profile from the backward iterations meets the profile from the forward iterations, the intersection is our desired HCSP.

5.4. Speed–Ceiling Profile ($V_h = V_{limits}$)

The speed–ceiling profile is the fastest speed profile under given conditions, which means that the train runs as fast as possible and travels with the minimal running time. A speed-ceiling profile can be made after all lines in steps 5.1–5.3 have been connected under maximum speed holding without coasting. The basic assumption of eco-driving is that the running time from the timetable should be greater than the minimal running time. The speed ceiling profile acts as the upper limit of possible strategies during strategy optimization, which can filter out part of the invalid control output alternatives and reduce the calculation load. Figure 11 presents the speed ceiling profile ($V_{Ceiling}$) based on a 5000 t freight train and railway line matrix (see Appendix C) of a test line.

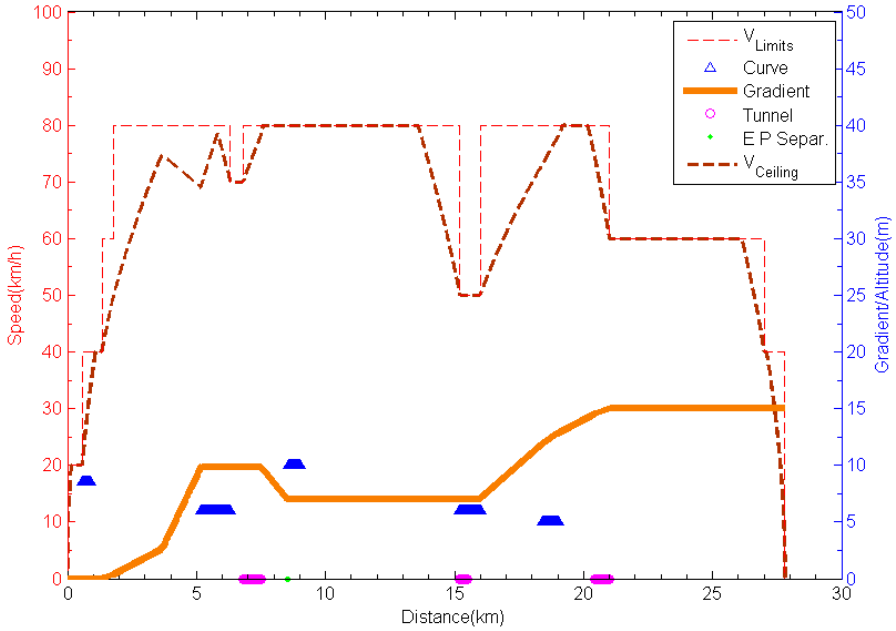

Figure 11. Speed ceiling profile diagram of a test line.

5.5. Adaptive Resolution of Holding Speed

If the scheduled running time is greater than the minimal running time in Section 5.4, moderate coasting will be necessary, and we need a proper speed holding mode to combine the acceleration and coasting mode. Therefore, the accurate calculation of the holding speed V_h is very important. This algorithm applies a resolution with adaptive step sizes to find the proper value of V_h.

Preliminarily set a value V_{h1} in accordance with the running time and distance, and then attempt to calculate whether the trip could be completed within the scheduled running time.

If the trip can be completed with some running time surplus, which is the most common situation, repeatedly reduce V_h with a step size ΔV_{h1} until the running time is sufficient. Then, return to the last round of reduction and repeatedly decrease V_h with a step size $\Delta V_{h2} = 0.1\Delta V_{h1}$ until the running time is sufficient. The step size should be repeatedly decreased in the same way until the precise requirement has been met.

If the trip cannot be completed within the scheduled running time, which means that the preset V_{h1} is not sufficiently large, increase V_h with adaptive step sizes in the same way.

5.6. Speed Reference Profile

The speed reference profile is the speed reference line for local speed profile optimization. It is the optimal speed profile if there is no steep track to interrupt the speed holding phase of the journey. Speed reference profile programing fully considers the operating constraints from the track and the locomotive. However, for sections with steep slopes, curves, tunnels, etc., where the traction characteristics of the locomotive are not sufficiently strong to maintain a constant speed, it merely maintains the holding speed as a reference of the local optimization of the next step. Hence, the speed profile outline and some of the switching points between different modes can be properly located. It distributes the running time over different sections according to the scheduled running time and journey distance. Here, a typical speed reference profile is sketched as the dotted blue line in Figure 12.

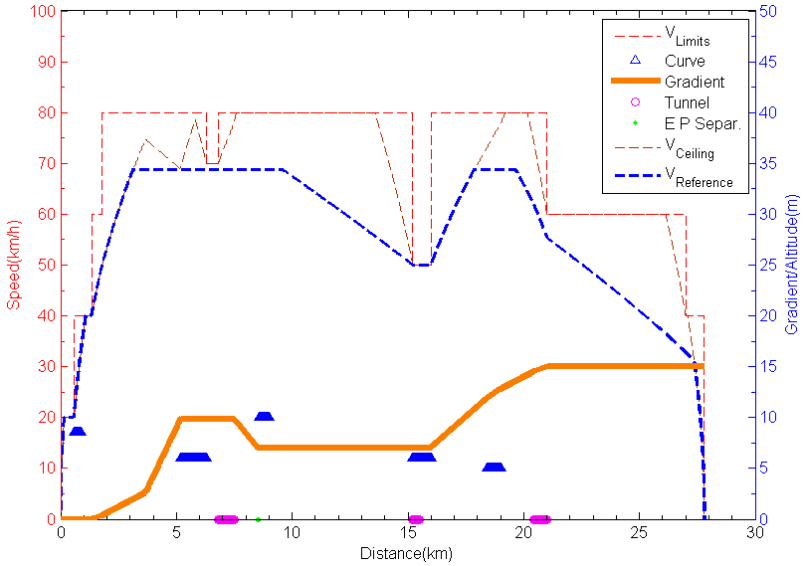

Figure 12. Speed reference profile diagram of a test line.

5.7. Local Approximation for Steep Tracks (Average Speed Equivalent Algorithm)

For a line with steep sections, the speed holding mode would be interrupted by phases of maximum power (steep uphill) or coasting (steep downhill). Scholars worldwide have performed substantial work on speed profile optimization on steep tracks, and some researchers have attempted to solve the problem using co-state equations, maximum principles, etc. However, these methods require multiple rounds of calculation before reaching a satisfactory solution, and the calculations are complex with high computational costs. More importantly, when we discuss energy efficiency, it should be based on a certain given running time as a precondition. Some studies, however, have not adequately eliminated the negative influence caused by local optimizations on global time allocation. This paper proposes an adaptive resolution-based average speed equivalent algorithm to quickly locate the switching points of motoring before travelling uphill and coasting before travelling downhill.

5.7.1. A Local Speed Profile Approximation Algorithm for Steep Uphill Slopes

Generally speaking, a train must accelerate with maximum power in advance to overcome a steep uphill section. How to obtain the correct HASP is then the key problem.

Taking references from drivers' manual operation, we attempt to turn the difficult global optimization problem into a much easier local optimization problem by maintaining the running time as constant as possible. The reason for this is similar to why we maintain the speed and running time as constant on non-steep track. The difference is that the train must suffer the extra resistance energy consumption caused by speed fluctuations. Taking the steep uphill slope in Figure 10 as an example, the gray line indicates the altitude of the railway line; and the slope of the gray line indicates the steep uphill slope.

First, it is necessary to define the upper bound and lower bound of the optimal strategies: There are three lines in the middle of the speed profile. The upper line is the upper bound of acceleration, which ensures that the speed returns to V_h after the train passes the slopes. The lower bound means that acceleration in advance is not needed; the locomotive uses its maximum power at the foot of the slope until the speed recovers toV_h. There are numerous potential strategies between the upper and lower bounds; the green line is our desired strategy and achieves an average speed equal to V_h. This means that the running time equals the time cost of a train running at a constant speed. To obtain the green line in Figure 13, our approach starts from the lower bound (blue line) in an adaptive resolution approach that is similar to what we discussed in Section 5.5.

$$\frac{x_{AHSP} - x_{HASP}}{t_{AHSP} - t_{HASP}} = V_h \tag{23}$$

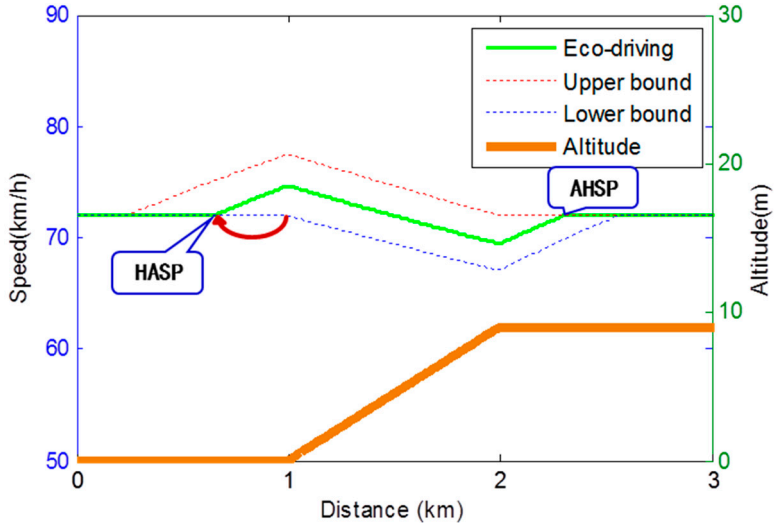

Figure 13. Diagram of the average speed equivalent algorithm for a 1 km steep uphill slope.

Why is the green line in Figure 13 the optimal strategy? To answer this question, we performed a comparative simulation of different operation strategies. Some related parameters used in the derivation are listed in Table 2.

Table 2. Subscripts, parameters, and variables used in the mathematical formulations.

Symbol	Definition
E_{SU_Stri}, E_{SU_Strj}	Energy consumption of the steep uphill slope in strategies i and j
$E_{Oth\_Stri}, E_{Oth\_Strj}$	Energy consumption of the trip except for the steep uphill slope in strategies i and j
Str_i, Str_j	Strategy i and strategy j
t_{HASP}, t_{AHSP}	Time of hold–accelerate and accelerate–hold switching points
T_{SU_Stri}, T_{SU_Strj}	Time cost of the steep uphill slope in strategies i and j
$T_{Oth\_Stri}, T_{Oth\_Strj}$	Time cost of the trip except for the steep uphill slope in strategies i and j
$v_{Stri}(x), v_{Strj}(x)$	Speed of position x in strategies i and j
$x_{HCSP}, x_{HASP}, x_{AHSP}$	Positions of *HCSP*, *HASP*, and *AHSP*

To show how the different HASPs impact the total energy consumption, we set x_1 as the starting point of the uphill slope, as shown in Figure 14a, which presents a close-up of the part of the speed profile near the slope, and we iterate x_{HASP} with a step size of 10 m. The energy consumption of each steep-uphill-pass strategy is collected and shown in Figure 14b.

Each blue line in Figure 14a indicates a speed profile of a steep-uphill-pass strategy. For any strategy Str_i andStr_j, $x_{HASPj} < x_{HASPi}$ means that Str_j switches to full power earlier than Str_i. Thus, we can say that $v_{Strj}(x) > v_{Stri}(x)$ during $x_{AHSPj} < x < x_{AHSPi}$. The basic resistance depends on the speed value; thus, we can say that the energy consumption during this section satisfies the relation $E_{SU\_Strj} > E_{SU\_Stri}$, whereas the time cost relation for these two strategies is $T_{SU\_Strj} < T_{SU\_Stri}$. Because the running time of the whole trip is scheduled, we obtain $T_{Oth\_Strj} > T_{Oth\_Stri}$, and $V_{h\_Strj} < V_{h\_Stri}$, as we can see in Figure 14a. A lower V_h also means a lower energy consumption; thus, we have $E_{Oth\_Strj} < E_{Oth\_Stri}$. For $E = E_{SU} + E_{Oth}$, it is difficult to say which strategy is more energy efficient.

Specifically, to pass a short, steep uphill slope, the energy consumption does not exhibit an obvious relationship in cases where full power is applied. What about cases with a long, steep uphill slope?

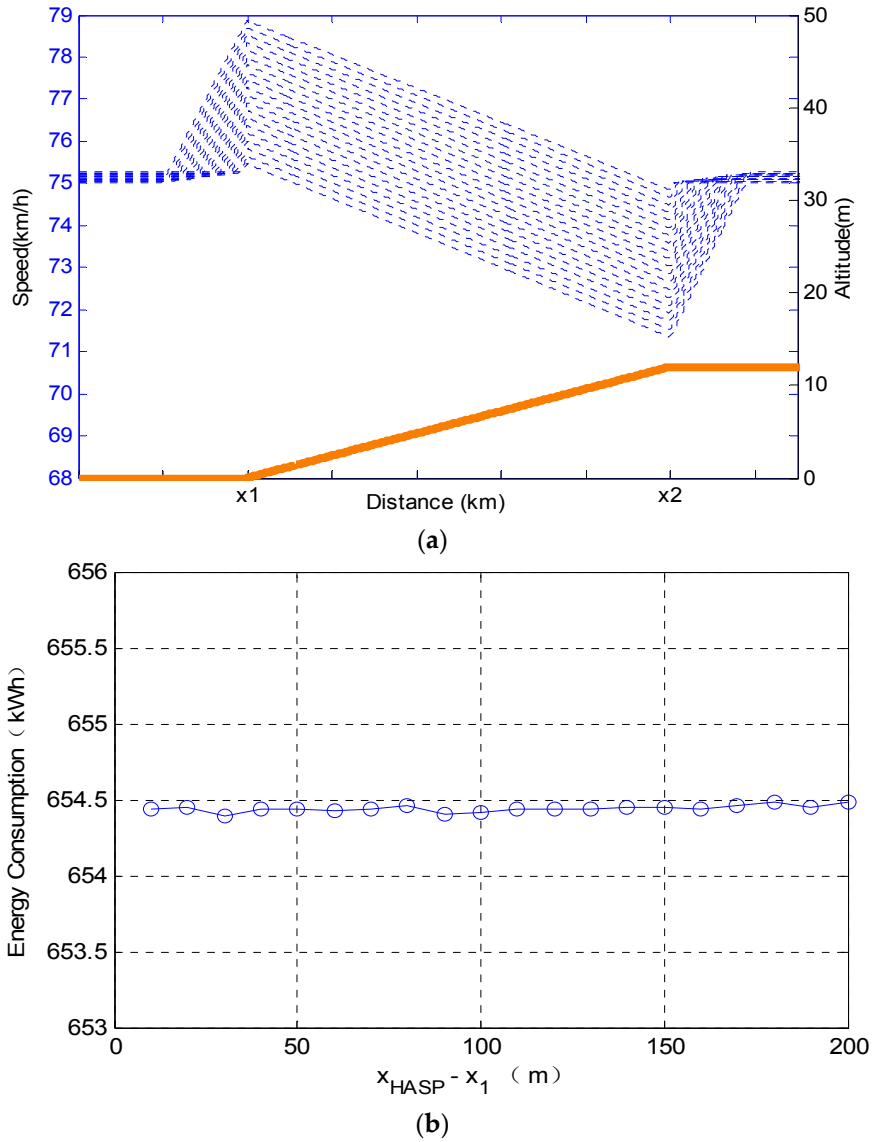

Figure 14. Comparison chart of different steep-uphill-pass strategies for a 1 km uphill slope. (**a**) Speed profiles of different strategies; (**b**) Energy consumptions of different strategies in (**a**).

Figure 15 shows the simulation of a test line, which has a long, steep uphill slope from $x_0 = 10$ km to $x_1 = 20$ km. As Figure 15b shows, the energy consumption on a long, steep uphill slope is more sensitive to HASP than on the shorter slopes, and it appears to be a convex function of $x_{HASP} - x_1$ for 0–2400 m. However, as shown in Figure 15a, the maximum speed at the foot of the uphill slope would be very high. The speed limit of freight trains in China is often 80 km/h, and a common cruise velocity is 75 km/h. Thus, there is no room for large accelerations in practice.

Most importantly, a train passing a steep section by the green line strategy in Figure 13 exhibits no obvious advantage compared with other strategies regarding energy consumption. Thus, why should the green line in Figure 13 be the optimal strategy? This is because its running time cost is equivalent to one for which the train passes with a holding speed V_h. This characteristic will help us transform the complex global optimization problem into a much simpler local optimization problem, greatly increasing the computational efficiency.

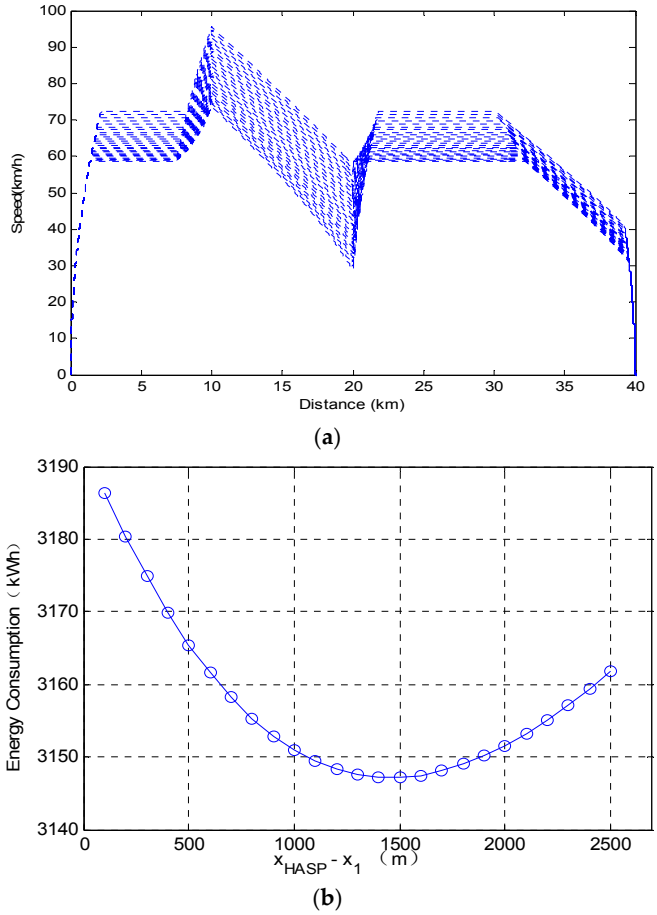

Figure 15. Comparison chart of different steep-uphill-pass strategies on a 10 km uphill slope. (**a**) Speed profiles of different strategies; (**b**) Energy consumptions of different strategies in (**a**).

5.7.2. Average Speed Equivalent Algorithm for Steep Downhill Track

In cases with steep downhill slopes, the component of the gravity force in the downhill direction is larger than the resistance, and the speed will increase even if the engine is turned off. Following the same idea as a steep uphill slope, we should find the proper coasting point and start to coast in advance before the steep downhill slope. The key is to also maintain the average speed equivalent to V_h. Figure 16 shows the local optimization of the speed profile of a steep downhill slope.

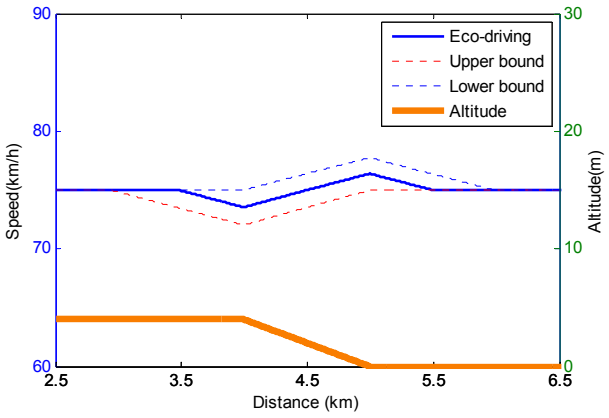

Figure 16. Diagram of the average speed equivalent algorithm for a steep downhill slope.

6. Case Study

Case 1. We ran a simulation of a test line; the results are shown in Figure 17, and the simulation results obtained using Dynamis 2.0 are shown in Figure 18 for comparison. Dynamis is a professional software package commercialized by the Institute for Transport, Railway Construction, and Operation of the University of Hanover. In general, the shape of our speed profile $V_{optimal}$ in Figure 17 is more reasonable. Braking mode is used only to stop the train at the destination. Broad speed holding sections in Figure 17 make speed tracking and dynamic adjustment easier to execute with fewer control mode switches. By comparing Figure 17 with Figure 18, we can see that Figure 17 is more reasonable, especially in the steep downhill section from 7.5 to 8.5 km and the speed limit slowdown sections after 15.2 km and 27 km, where the braking mode should be replaced by coasting in advance. The table above in Figure 18 shows that the 2151.5 s trip costs 2179.6 kWh of energy with 271.5 kWh of braking energy being sent back to the electric power network, and the calculation time is approximately 30 s. The optimized speed profile in Figure 17 shows that the trip fully utilizes the given 2200 s running time, consuming a total of 1886.13 kWh of energy with 70.88 kWh of braking energy being regenerated. The calculation time for the simulation in Figure 17 is approximately 10 s for an ordinary desktop computer with Matlab R2012a.

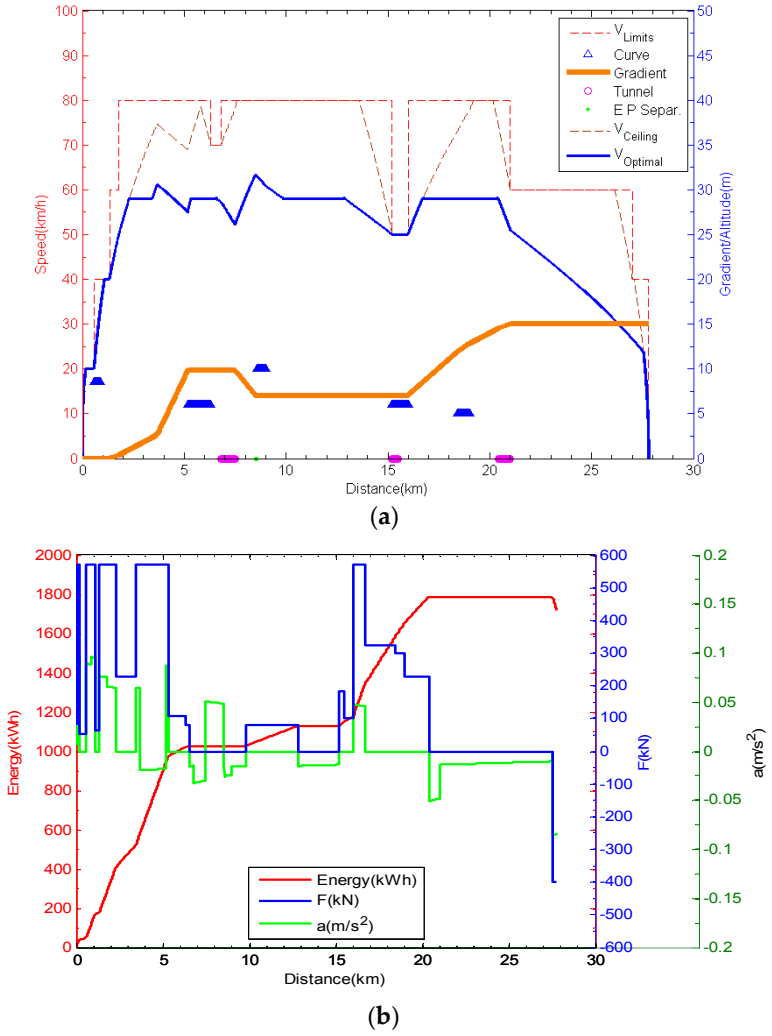

Figure 17. Simulation of speed profile programing in a test line with both steep uphill and downhill sections. (**a**) Diagram of the optimized speed profile; (**b**) Acceleration, traction force, and energy consumption of (**a**).

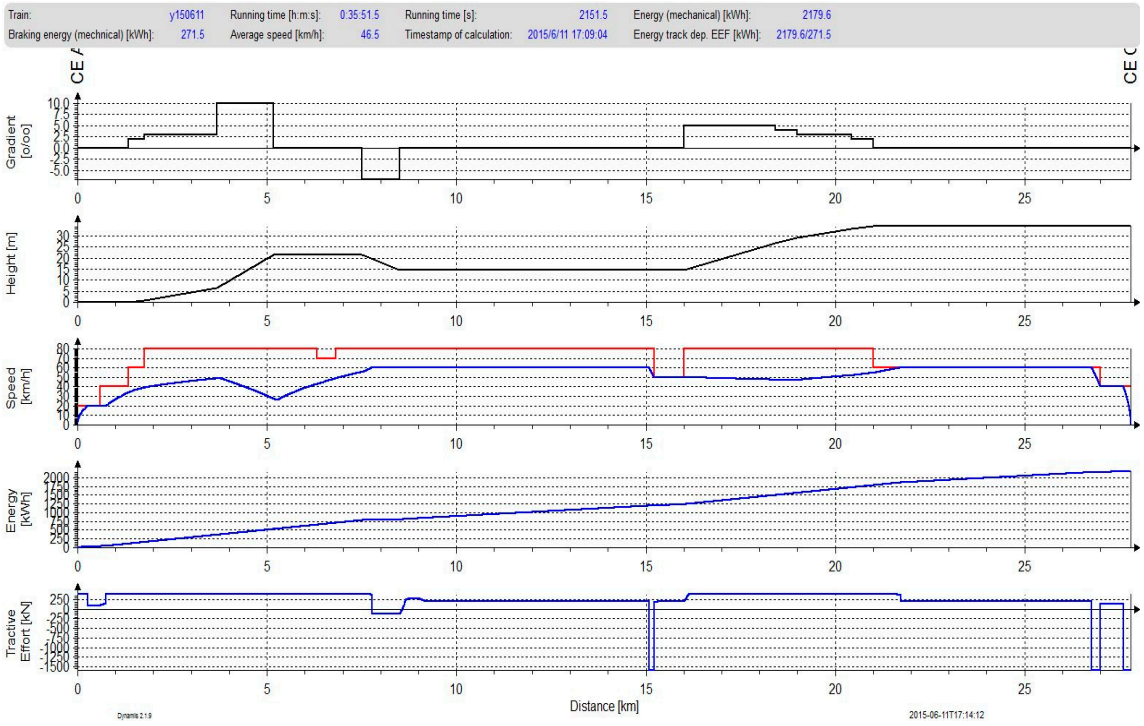

Figure 18. Speed profile optimization by Dynamis 2.0.

The algorithm that we propose should be suitable for urban trains and passenger trains after some necessary transformations; see the following Case 2.

Case 2. As is introduced in the literature review, Lu et al. from the University of Birmingham performed an excellent work on speed profile optimization using GA (Figure 19a), ACO (Figure 19b), and DP (Figure 19c) (Lu, 2011). We performed a simulation as shown in Figure 20 with the same line conditions to show that the adjusted algorithm is suitable for the eco-driving strategy optimization of an urban train whose line conditions are usually simpler. The calculation times of Lu's cases in Figure 19 are 1550.5 s, 552.3 s, and 2431.8 s. Our new method can draw a set of speed profiles with different given running times as shown in Figure 20, in only a few seconds.

Figure 19. Speed profile optimization by ACO (**a**); GA (**b**); and DP (**c**) of Lu (2011).

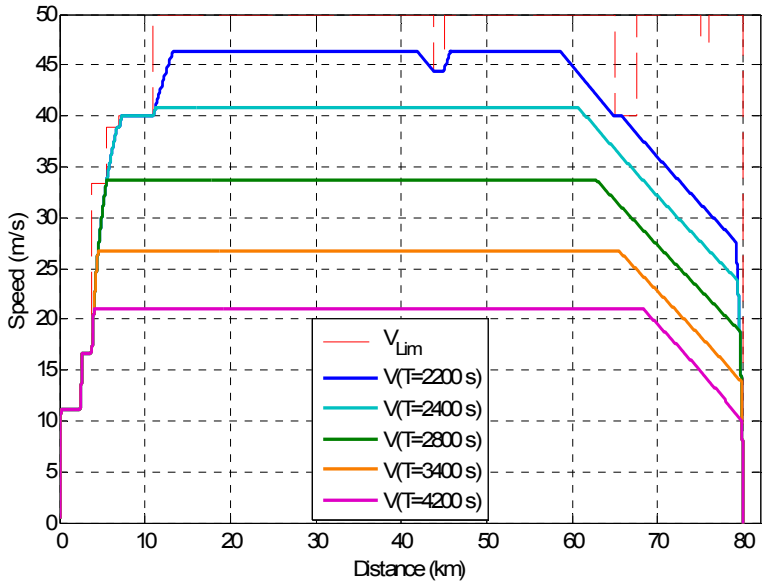

Figure 20. Comparative analysis with Figure 19 using this paper's proposal.

Case 3. Constrained by the freight train's mechanical system and electrical system characteristics, the target speed profile of ATO should be stable, with a low change frequency and a wide range of speed holding modes. According to the existing ATO of a freight train, this work builds a simulation platform as shown in Figure 21, in which the speed controller is designed in a Simulink model. The speed tracking effect can be simulated on the platform to examine the quality of the speed profile obtained from this paper's proposed algorithm.

As shown in Figure 22, the optimized speed profile can be tracked quite well, except for the proximity of the switching points. Overshoots are found at approximately t = 480 s and t = 800 s.

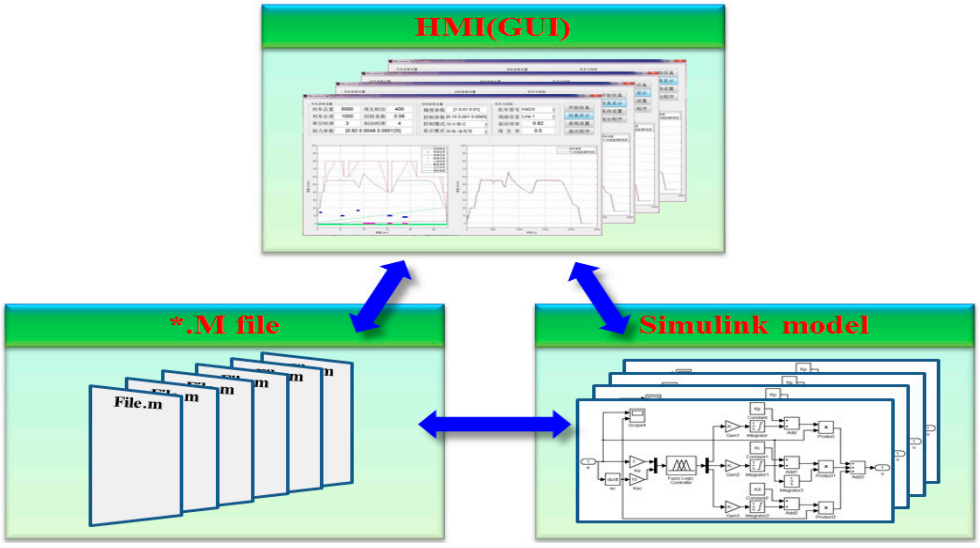

Figure 21. Framework of the simulation platform.

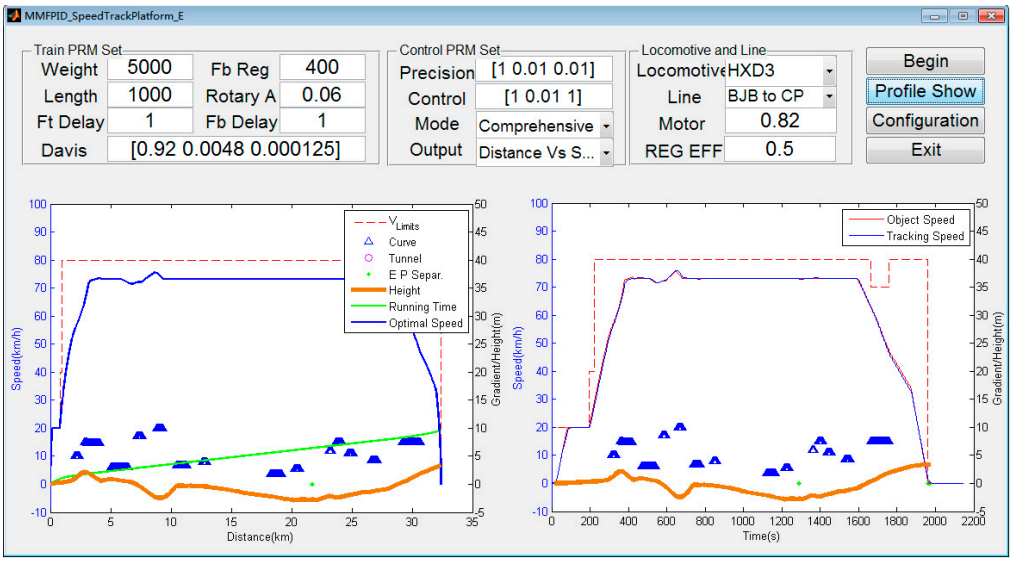

Figure 22. Speed tracking effect evaluation under the simulation platform: From Beijingbei, China to Changping, China.

7. Conclusions and Future Work

According to the characteristics of an electrical locomotive with regenerative braking, this paper proposes a new algorithm for train speed profile optimization. The novelty lies in the following results.

First, the paper demonstrates that under a certain calculation precision, there is an optimal coast-brake switching region, not just a point, where a train should be switched from coasting mode to braking mode.

Second, the paper analyses the influence on energy consumption caused by regenerative braking in the optimal coast-brake switching region and studies the approximate linear relationship between the optimal switching region and the regeneration efficiency for speed profile optimization. The influence of running time is also analyzed. From these analyses, we obtain a conclusion that the most important aspect of energy-efficient train operation is to fully utilize the scheduled running time.

Third, with the section running time held relatively stable, this paper proposes transforming the complex global optimization problem into a simpler local optimization problem and presents the average speed equivalent algorithm for the local speed profile approximation of short, steep track.

The proposed algorithm is suitable for developing a fast and feasible speed profile approximation system. Practitioners and engineers can apply the algorithm to ATO system design. Future research work should focus on creating more efficient algorithms of online speed profile approximation based on the algorithm proposed in this paper. In addition, a specific study should be dedicated to tracking the speed profile precisely.

Acknowledgments: The authors would like to thank all reviewers for their help and valuable comments and the contributions of Yong Yang, Xiukun Wei, Zhuoyue Li, Youran Lv, and Jinglin Zhang for this paper. This work was supported in part by the National Key Technology Research and Development Program of the Ministry of Science and Technology of China (Project No. 2013BAG24B03), the National Natural Science Foundation of China (Project No. 61603306, No. 61305019), and the Research Foundation of Education Bureau of Jiangxi Province (No. GJJ150620).

Author Contributions: Limin Jia and Jie Yang conceived and designed the experiments; Jie Yang and Yunxiao Fu performed the experiments; Shaofeng Lu and Ji Ge analyzed the data; Jie Yang and Shaofeng Lu wrote the paper.

Conflicts of Interest: The authors declare no conflict of interest.

Appendix A. Mathematical Basis

The literature on energy-efficient train operation always has certain application restrictions, generally focusing on particular engineering contexts and specific scenarios and goals. Based on the multiple optimization objectives for energy-saving freight train operation, this paper systematically integrates relevant research outcomes as proposed by Howlett [5], Vu [6], Lu [11], and Bai [29]. Some related parameters used in the derivation are listed in Table A1.

Table A1. Subscripts, parameters, and variables used in the mathematical formulations.

Symbol	Definition
c_i	Resultant force per unit mass of time step i
e_{net_i}	Energy input from the electric power network of time step i
$\underline{f(v,u)}$	Traction force per unit mass arc (v,u)
$\overline{F(v,u)}$	Maximum traction force per unit mass arc (v,u)
$\overline{F}_{Adhesion}$	Maximum adherence force per unit mass
i_j	Track gradient additional resistance per unit mass
L_{train}, L_{tunnel}	Length of the train and the tunnel
M	Mass of the train
$P_{auxiliary}$	Power of auxiliary systems
S	Trip distance
t_0, t_S, T	Time of starting point, time of end point, scheduled running time
θ	Central angle of the curve
ρ_a, ρ_b, ρ_c	Empirical constants of rolling resistance, track resistance, and aerodynamic resistance
$\rho_{curve}, \rho_{tunnel}$	Empirical constants of curve resistance and tunnel resistance
$\eta_{mechanical}, \eta_{power\_sys}, \eta_{motor}$	Efficiency of mechanical system, power system, and motor
$\omega_0, \omega_j, \omega_{curve}, \omega_{tunnel}$	Basic resistance, additional resistance, curve additional resistance, and tunnel additional resistance per unit mass
Δt	Time step size

Ideally, the discrete motion of a point-mass train can be formulated as

$$\begin{aligned} &c = f_t(v,u) - r(v) - \omega_j(x,v) - B(u) \\ &v_0 = v_S = 0 \\ &t_0 = 0, t_S = T \end{aligned} \tag{A1}$$

Force analysis of the train operation c is very complex, and it can be roughly divided into the traction force f, braking force b_0, and resistance w. The traction force does not work with the braking force at the same time. The resistance w can be divided into the basic resistance r and an additional resistance w_j. The additional resistance w_j can also be divided into track gradient additional resistance i_j, curve additional resistance w_r, and tunnel additional resistance w_t.

The basic resistance is usually given by the Davis equation

$$r(v) = \rho_a + \rho_b \cdot v + \rho_c \cdot v^2 \tag{A2}$$

The additional resistance is

$$\omega_j(x,v) = i_j(x) + \omega_{curve}(x,v) + \omega_{tunnel}(x,v) \approx i_j(x) + \frac{\rho_{curve} \cdot \theta}{L_{train}} + \rho_{tunnel} \cdot L_{tunnel} \tag{A3}$$

The traction and braking characteristics are a set of lines that show the traction force changing with changing speed. The traction force during motion and the braking force during regenerative braking can be calculated using piecewise interpolation according to the traction and braking characteristics of corresponding locomotives. Electric braking in an HXD3 locomotive is regenerative. The traction motor becomes a generator during regenerative braking and converts the kinetic energy of the train into electrical energy, which is sent back to the electric network through the converter and pantograph.

The traction energy in time step i is

$$e_{traction\_i} = \frac{1}{\eta_{mechanical}} \cdot f(v_i, u_i) \cdot v_i \cdot \Delta t \tag{A4}$$

$$f(v_i, u_i) = \frac{\min\left\{\overline{F(v_i, u_i)}, M \cdot \overline{a}, \overline{F_{adhesion}}\right\}}{M \cdot g} \tag{A5}$$

Considering all factors of motor efficiency and the energy consumption of auxiliary systems, the total energy input from the net in each time step i is

$$e_{net\_i} = \frac{1}{\eta_{power\_sys}} \cdot \left(\frac{e_{traction\_i}}{\eta_{motor}} + P_{auxiliary} \cdot \Delta t\right) \tag{A6}$$

Appendix B. Operation Constraints

Some related parameters used in the derivation are listed in Table B1.

Table B1. Subscripts, parameters, and variables used in the mathematical formulations.

Symbol	Definition
$a_i, \underline{a}, \overline{a}$	Acceleration at time step *i*, minimum acceleration, and maximum acceleration
$s_{arrive}, \overline{s_{error}}$	Position of the parking point, and maximum acceptable parking error
$t_{arrive}, \overline{t_{error}}$	Parking time, and maximum acceptable parking time error
$v_{\lim}, v'_{\lim}, v''_{\lim}$	Speed constraint, static speed constraint, and dynamic speed constraint
$\lambda_{Ja}, \lambda_{Jv}, \lambda_{Jt}, \lambda_{Js}$	Weight of the acceleration, speed limit constraint, on time, and arrival location satisfactory degree function

Acceleration constraints: The safety of a running train and of a braking train mainly depends on the train's acceleration and its changing rate—i.e., its jerk rate. A strong acceleration or jerk rate will lead to damage to the couplers and goods. Here, we limit its maximum and minimum value as

$$\underline{a} \le a_i \le \overline{a} \tag{B1}$$

Accurate parking: Accurate parking means appropriate braking to park at the exact location and time. Accurate parking reflects the punctuality degree of train operations, and guarantees the operational efficiency of railway transportation. Here, we limit the maximum distance and time deviation as

$$|s_{arrive} - S| \le \overline{s_{error}} \tag{B2}$$

$$|t_{arrive} - T| \le \overline{t_{error}} \tag{B3}$$

Speed constraints: Static speed constraints of the railway line and the dynamic speed constraints during train-following operations can be formulated as (Bai 2010)

$$\begin{aligned} &0 \le v_i \le v_{\lim} \\ &v_{\lim} = \min(v'_{\lim}, v''_{\lim}) \end{aligned} \tag{B4}$$

Objective function: The objective function used to judge which strategy should be adopted during online monitoring is given as

$$J = \sum_{i=1}^{n} e_{net\_i} + \lambda_{Ja} \sum_{i=1}^{n} \mu_a(a_i) + \lambda_{Jv} \sum_{i=1}^{n} \mu_v(v_i) + \lambda_{Jt} \mu_t(t_{arrive} - T) + \lambda_{Js} \mu_s(s_{arrive} - S) \tag{B5}$$

where $\mu_a(a_i)$ is a function used to calculate the cost arising from an acceleration constraint violation, $\mu_v(v_i)$ is a function used to calculate the cost arising from a speed limit constraint violation, $\mu_t(t_{arrive} - T)$ is a function used to reflect the cost of when the train operation deviates from the scheduled timetable, and $\mu_s(s_{arrive} - S)$ is a function that represents the cost due to the difference between the arrival location and the designated arrival position. λ_{Ja}, λ_{Jv}, λ_{Jt}, λ_{Js} are the weights of previously described functions, and e_{net} is the energy input from the net, whose weight is $\lambda_{Je} = 1$.

Appendix C. Construction of the Railway Line Matrix

Through information acquisition and analysis using a LKJ2000 monitoring device, this paper designs a program module of a railway line matrix, which includes distance, speed limitations, curve radius, gradient, tunnel, electric phase separation, and other information. The matrix is indexed by a distance mark, containing the information needed in the calculations of i_j, ω_{curve}, ω_{tunnel}. Figure C1 shows some of the information from the railway line matrix of a test line.

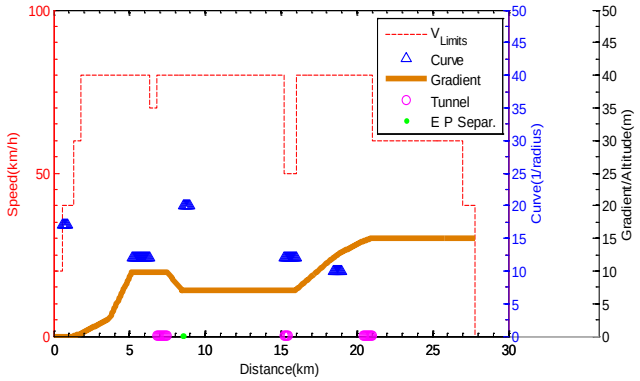

Figure C1. Graphical display of the railway line matrix.

As shown in Figure C1, the red line is the speed limit. The blue trapezoid formed by many triangles overlapping indicates the route curvature, and their values on the blue y-axis come from the inverse of the curve radius plus 1200. The brown line indicates the altitude of the track and reflects the gradients along the line. The pink line formed by many overlapping circles indicates the presence of tunnels. The green dot indicates the presence of electric phase separation, which means that approximately 75 m of lines are without power supply. To make the figure more concise, we often omit the y-axis indicating curves and gradients in the following figures.

References

1. Sidelnikov, V. Computation of optimal controls of a railroad locomotive. *Proc. State Railw. Res. Inst.* **1965**, *2*, 52–58.
2. Cheng, J.; Howlett, P. A note on the calculation of optimal strategies for the minimization of fuel consumption in the control of trains. *IEEE Trans. Autom. Control* **1993**, *38*, 1730–1734. [CrossRef]
3. Cheng, J. Analysis of Optimal Driving Strategies for Train Control Problems. Ph.D. Thesis, University of South Australia, Adelaide, Australia, 1997.
4. Howlett, P. The optimal control of a train. *Ann. Oper. Res.* **2000**, *98*, 65–87. [CrossRef]
5. Howlett, P.G.; Pudney, P.J. *Energy-Efficient Train Control*; Springer Science & Business Media: New York, NY, USA, 2012.
6. Vu, X. *Analysis of Necessary Conditions for the Optimal Control of a Train: New Necessary Conditions for Energy-Efficient Train Control*; VDM Publishing: Berlin, Germany, 2009.
7. Albrecht, A.; Howlett, P.; Pudney, P.; Vu, X.; Zhou, P. The key principles of optimal train control—Part 1: Formulation of the model, strategies of optimal type, evolutionary lines, location of optimal switching points. *Transp. Res. B Methodol.* **2015**, in press. [CrossRef]

8. Albrecht, A.; Howlett, P.; Pudney, P.; Vu, X.; Zhou, P. The key principles of optimal train control—Part 2: Existence of an optimal strategy, the local energy minimization principle, uniqueness, computational techniques. *Transp. Res. B Methodol.* **2015**, in press. [CrossRef]
9. Khmelnitsky, E. On an optimal control problem of train operation. *IEEE Trans. Autom. Control* **2000**, *45*, 1257–1266. [CrossRef]
10. Liu, R.R.; Golovitcher, I.M. Energy-efficient operation of rail vehicles. *Transp. Res. A Policy Pract.* **2003**, *37*, 917–932. [CrossRef]
11. Lu, S. Optimising Power Management Strategies for Railway Traction Systems. Ph.D. Thesis, University of Birmingham, Birmingham, UK, 2011.
12. Lu, S.; Weston, P.; Hillmansen, S.; Gooi, H.B.; Roberts, C. Increasing the regenerative braking energy for railway vehicles. *IEEE Trans. Intell. Transp. Syst.* **2014**, *15*, 2506–2515. [CrossRef]
13. Lu, S.; Wang, M.Q.; Weston, P.; Chen, S.; Yang, J. Partial Train Speed Trajectory Optimization Using Mixed-Integer Linear Programming. *IEEE Trans. Intell. Transp. Syst.* **2016**. [CrossRef]
14. Miyatake, M.; Matsuda, K. Energy Saving Speed and Charge/discharge Control of a Railway Vehicle with On-board Energy Storage by Means of an Optimization Model. *IEEJ Trans. Electr. Electron. Eng.* **2009**, *4*, 771–778. [CrossRef]
15. Miyatake, M.; Ko, H. Optimization of Train Speed Profile for Minimum Energy Consumption. *IEEJ Trans. Electr. Electron. Eng.* **2010**, *5*, 263–269. [CrossRef]
16. Ho, T.K.; Mao, B.H.; Yuan, Z.Z.; Liu, H.D.; Fung, Y.F. Computer simulation and modeling in railway applications. *Comput. Phys. Commun.* **2002**, *143*, 1–10. [CrossRef]
17. Sheu, J.W.; Lin, W.S. Energy-saving automatic train regulation using dual heuristic programming. *IEEE Trans. Veh. Technol.* **2012**, *61*, 1503–1514. [CrossRef]
18. Yasunobu, S.; Miyamoto, S. Automatic train operation system by predictive fuzzy control. *Ind. Appl. Fuzzy Control* **1985**, *1*, 1–18.
19. Jia, L. Intelligent Distributed Railway Traffic Control Based on Fuzzy Decision making. *China Railw. Sci.* **1994**, *62*, 255–268.
20. Bai, Y.; Ho, T.K.; Mao, B.; Ding, Y.; Chen, S. Energy-efficient locomotive operation for Chinese mainline railways by fuzzy predictive control. *IEEE Trans. Intell. Transp. Syst.* **2014**, *15*, 938–948. [CrossRef]
21. Chang, C.S.; Sim, S.S. Optimising train movements through coast control using genetic algorithms. *IEE Proc. Electr. Power Appl.* **1997**, *144*, 65–73. [CrossRef]
22. Wong, K.K.; Ho, T.K. Dynamic coast control of train movement with genetic algorithm. *Int. J. Syst. Sci.* **2004**, *35*, 835–846. [CrossRef]
23. Lu, Q.; Feng, X.; Wang, Q. Energy-saving optimal control of following trains based on genetic algorithm. *J. Southwest Jiaotong Univ.* **2012**, *2*, 10–17.
24. Li, X.; Lo, H.K. An energy-efficient scheduling and speed control approach for metro rail operations. *Transp. Res. B Methodol.* **2014**, *64*, 73–89. [CrossRef]
25. Huang, Y.; Ma, X.; Su, S.; Tang, T. Optimization of Train Operation in Multiple Interstations with Multi-Population Genetic Algorithm. *Energies* **2015**, *8*, 14311–14329. [CrossRef]
26. Lin, F.; Liu, S.; Yang, Z.H.; Zhao, Y.; Yang, Z.P.; Sun, H. Multi-Train Energy Saving for Maximum Usage of Regenerative Energy by Dwell Time Optimization in Urban Rail Transit Using Genetic Algorithm. *Energies* **2016**, *9*, 208. [CrossRef]
27. Yin, J.; Chen, D.; Li, L. Intelligent train operation algorithms for subway by expert system and reinforcement learning. *IEEE Trans. Intell. Transp. Syst.* **2014**, *15*, 2561–2571. [CrossRef]
28. Domínguez, M.; Fernández-Cardador, A.; Cucala, A.P.; Gonsalves, T.; Fernández, A. Multi objective particle swarm optimization algorithm for the design of efficient ATO speed profiles in metro lines. *Eng. Appl. Artif. Intell.* **2014**, *29*, 43–53. [CrossRef]
29. Bai, Y. Modeling and Real-time Algorithm on Energy-efficient Operation for Freight Train with Diesel Locomotive. Ph.D. Thesis, Beijing Jiaotong University, Beijing, China, 2010.

© 2016 by the authors; licensee MDPI, Basel, Switzerland. This article is an open access article distributed under the terms and conditions of the Creative Commons Attribution (CC-BY) license (http://creativecommons.org/licenses/by/4.0/).